Nonlinear transport through coupled double-quantum-dot systems

R. Kotlyar and S. Das Sarma

Department of Physics, University of Maryland, College Park, Maryland 20742-4111

(Received 4 December 1996; revised manuscript received 27 June 1997)

We investigate transport via sequential tunneling through a semiconductor double quantum dot structure by combining a simple one-dimensional microscopic quantum confinement model with a Mott-Hubbard-type correlation model. We calculate nonperturbatively the evolution of the Coulomb blockade oscillations as a function of the interdot barrier conductance, obtaining qualitative agreement with the experimental data over the whole tunneling regime from the weak-coupling individual dot to the strong-coupling coherent double-dot molecular system. [S0163-1829(97)06844-6]

I. INTRODUCTION

By tuning the tunnel barrier between the individual dots of a voltage-biased semiconductor double-quantum-dot system, it has recently been possible[1] to observe the formation of an artificial double-dot molecule (with each dot as its atomic constituents) in Coulomb blockade transport experiments.[1-3] As the interdot tunneling is increased, the series of linear conductance peaks of the two individual near-identical dots[1-3] changes continuously to a series of split peaks which then form a well-defined Coulomb blockade oscillation series with twice the individual Coulomb blockade period. This period doubling transition in the Coulomb blockade oscillations closely follows the energetics of the transition of two fully isolated dots into a single composite dot due to enhanced interdot tunneling. This transition raises important general questions on how the parameters that can be uniquely defined for the isolated system would renormalize in the transparent composite system. For example, to add an electron to a single dot requires energy in excess of the intradot interaction energy u_{11}. For two isolated dots in series in a double-dot system, supplying the required energy u_{11} corresponds to the addition of one electron to each of the dots. With the increased ''transparency'' of the system due to enhanced tunneling, the energy u_{11} required to add an electron changes as the doubling in the periodicity of the linear conductance Coulomb peaks demonstrates. The pertinent theoretical question is how to characterize the increased ''transparency'' of the composite system. The classical capacitive charging model attributes this transition to the interdot electrostatic coupling energy u_{12}. In this model each dot is considered to contain an integer number of electrons. The splitting of the individual Coulomb blockade peak is proportional to the interdot coupling u_{12}. The saturation of the splitting in the strong-coupling limit is explained by the increase of u_{12} to the value of $u_{11}/2$ with all the other system parameters assumed constant.[1] The energy u_{12} is taken to arise from the capacitive coupling between the two dots, which is classically determined by the fixed geometrical arrangement of the dots. Thus, within the classical capacitive charging model the fixed geometrical arrangement of the two dots in the experimental system provides no physical reason for the increase of u_{12} necessary to account for the saturation of the observed peak splitting. It has also been noted[1] that the

classical capacitance values needed to quantitatively explain the observed peak splitting are unphysically high.

A recent fully quantum theory[4,5] of charge fluctuations between the two dots formulates the double-dot problem in terms of the dimensionless interdot conductance per tunneling channel $g = G_{int}/(N_{ch}e^2/h)$ and the number of interdot tunneling channels N_{ch}. In the limit of the tunneling bandwidth being much larger than the intradot charging energy, each dot is treated as an infinite charge reservoir for the other dot. A perturbation analysis in g or in $(1-g)$ reproduces the weak and strong interdot coupling limits of the peak splitting. This multichannel perturbative analysis does not apply in the intermediate regime where $0 \ll g \ll 1$. The charge fluctuation perturbative analysis has not yet been extended to the nonlinear transport regime, which is a main focus of our work.

In this paper we study the transition from degenerate one-dot Coulomb blockade oscillation to the coherent molecular double-dot oscillation by using a two-site generalized Mott-Hubbard model within a simple physically motivated microscopic confinement potential describing the double-dot system. A Hubbard-type model of linear transport through the single-particle states of quantum dots[6-8] predicts the distinct phases in the conductance pattern characterized by an increase of the interdot tunneling strength t. In the strong tunneling limit the Mott-Hubbard insulator-metal transition opens a transmission channel through an array of quantum dots.[6] To characterize the dependence of the Hubbard model parameters on the value of the interdot conductance g, we use a one-dimensional phenomenological step-well model for the confinement potential profile of the double-dot system. Using the values of the Mott-Hubbard parameters determined by our model confinement potential for all values of the interdot conductance g we calculate the nonlinear current through the double-dot system for the whole range of the interdot coupling in the system. Thus our Mott-Hubbard approach to the double-dot system is in the spirit of the molecular-orbital theories that are widely used in chemistry. Our *nonperturbative* calculation is complementary in nature to the existing perturbative[4,5] analyses of the problem: in contrast to the multichannel continuum of states assumed in Refs. 4 and 5, and we use a finite number of single-particle states participating in the conduction through the double-dot system. Our model should be regarded as a simple nonper-
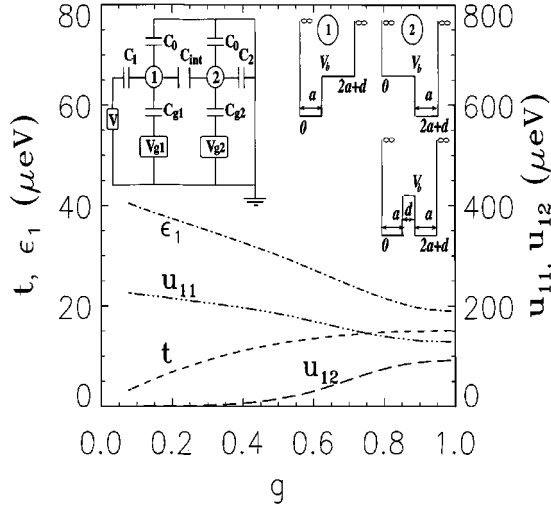
FIG. 1. Variation of the Hubbard model parameters u_{11}, u_{12}, t, and ε_1 with soft interdot conductance g. The conductance g is in units of $2e^2/h$. Insets: (left) the equivalent circuit of the double-dot system under study: the values of the capacitances $C_1 = C_2 = 38aF$, the other parameters are defined in the text; (right) the step-well model as defined in the text.

turbative phenomenological picture of the double-dot system in the limit of few conducting channels. In spite of this picture's simplicity, our calculation reproduces qualitatively the main experimental observations for both linear and nonlinear transport experiments. Our calculated finite temperature suppression of the linear current also agrees qualitatively with the experimental observation.[2]

The rest of the paper is organized as follows. We describe our Mott-Hubbard molecular-orbital model in Sec. II, also explaining our transport calculation within the master equation formalism. Our phenomenological double-dot confinement potential and the associated microscopic calculation of the Mott-Hubbard parameters are described in Sec. III. Sections IV and V give our calculated linear and nonlinear transport results, respectively, and we conclude in Sec. VI.

II. MODEL

The capacitive model of the experimental circuit configuration for the double-dot system[1–3] is shown in Fig. 1. We consider a symmetrical configuration of two identical GaAs dots with the same electrostatic couplings to the common back gate and to the bias leads, i.e., $C_{g1} = C_{g2} = C_g$, $C_1 = C_2 = C$, $V_{g1} = V_{g2} = V_g$, and common self-capacitances C_0. The interdot capacitor with the capacitance C_{int} provides the electrostatic coupling between the two dots. Following the experiments, we set an asymmetric bias across the system, i.e., $V_1 = V$, $V_2 = 0$. We express the electrostatic part of the free energy of the system using the classical capacitance matrix[9] formalism. In the usual final step of going into the quantum-mechanical description we replace the classical excess charge on a dot by the charge-density operator. Then the operator for the electrostatic free energy of the coupled system of the double dot and leads is

$$F^e = u_{11}(\hat{N}_1^2 + \hat{N}_2^2) + u_{12}\hat{N}_1\hat{N}_2 + eV(x_{b1}\hat{N}_1 + x_{b2}\hat{N}_2)$$
$$+ eV_g x_g(\hat{N}_1 + \hat{N}_2). \tag{1}$$

In Eq. (1) the Hubbard parameters are expressed through the elements of the capacitance matrix, i.e.,

$$u_{11} = e^2\frac{C_\Sigma}{2\delta}, \quad u_{12} = e^2\frac{C_{int}}{\delta}, \quad x_g = \frac{Cg}{e^2}(2u_{11} + u_{12}),$$

$$x_{b1} = \frac{C}{e^2}(2u_{11}), \quad x_{b2} = \frac{C}{e^2}(u_{12}),$$

where $C_\Sigma = C_0 + C_g + C + C_{int}$, and $\delta = C_\Sigma^2 - C_{int}^2$. We assume that the characteristic size a of each dot is much greater than the Bohr radius a_B of the bulk GaAs material. This allows us to use the effective-mass band description of the electron energies within a dot. All electron-electron interaction and lattice effects of a *neutral* dot are absorbed in the electron effective mass m^*. The band of interest in each neutral dot is the empty GaAs conduction band near its zone minimum. The bottom of the conduction band, considered to be the same in all GaAs electrodes in the system, is taken as the reference. Due to quantum confinement in the dot the continuous conduction band for an excess quasiparticle becomes a discrete series of single-particle energy levels ε_α, where α denotes the confined single-particle state ψ_α including spin. We consider spin-degenerate single-particle levels in the dot. The quasiparticles are allowed to tunnel between the single-particle states in the two dots with the tunneling amplitude t_α. In the occupation number second-quantized basis of single-particle states ψ_α we can write the total free-energy operator, including the kinetic energy in each dot and the tunneling energy, as

$$F^0 = F^e + \sum_{i=1,2,\alpha} \varepsilon_{i\alpha}c^\dagger_{i\alpha}c_{i\alpha} - \sum_\alpha (t_\alpha c^\dagger_{1\alpha}c_{2\alpha} + \text{H.c.}). \tag{2}$$

The indices 1,2 denote the spatial positions of the two dots, and $\hat{N}_i = \Sigma_\alpha c^\dagger_{i\alpha}c_{i\alpha}$ is the density operator, where $c^\dagger_{i\alpha}(c_{i\alpha})$ is a creation (annihilation) operator for a quasiparticle on the ith dot in a state α. Thus the applied bias voltage V modifies the potential landscape of the double dot by lowering the intradot single-particle energies through the capacitive coupling to the bias lead terms in Eq. (2). The gate voltage V_g plays the role of the chemical potential, and determines the total number of excess charges in the system at equilibrium. This Hamiltonian describes the two-dot system as a single coherent system at any strength of tunneling between the dots. As mentioned in the Introduction, this is exactly the spirit of the molecular-orbital theory in quantum chemistry, which we are adapting here for an artificial two-dot quantum molecule.

The double dot is isolated from the leads so that it is coupled to them only electrostatically and through (very weak) tunneling matrix elements $t_\alpha^{1,2}$. The conductance of the dot to the leads $G_{lead} = 0.02e^2/h(\ll e^2/h)$ is kept constant throughout. (The lead-dot tunneling strengths $t_1^{1,2} \sim \varepsilon_1[G_{lead}/(2e^2/h)]^{1/2}$ are estimated to be 3 μeV.) The tun-

neling hybridization energy between the double-dot and the bias leads is treated as a weak perturbation H_T:

$$H_T^{1,2} = \sum_{k\alpha} (t_\alpha^{1,2} c^\dagger{}_k c_{1,2\alpha} + \text{H.c.}), \qquad (3)$$

where the index k denotes a quasiparticle state in the leads.

Using Eqs. (1)–(3) we calculate the finite temperature current through the double dot system. We use the master equation approach and generalize the existing single-dot formalism[10,9] to calculate the current through the double dot, treating it as a single system described by Eqs. (1)–(3), under the assumptions of sequential tunneling $[kT \gg \hbar\Gamma = \hbar(\Gamma^1 + \Gamma^2)]$ and weak coupling to the outside leads. Our master equation based transport calculation should be valid within our model provided that the level separation ΔF in the double dot system is much less than the width of the transmission resonance $\hbar(\Gamma^1 + \Gamma^2)$, where Γ^1 (Γ^2) are the tunneling rates from the double dot through the first (second) junction. We consider the energy relaxation time τ to be much smaller than the lifetime of a quasiparticle in the double dot, i.e. $\tau \ll 1/\Gamma$. Similar to a single-dot[10] system, the probability distribution for the double dot to be in one of its excited states retains its equilibrium form, whereas the probability $P_{N_{\text{TOT}}}$ to find N_{TOT} number of quasiparticles in the double dot is determined by a stationary solution of the kinetic equation. The current through the double dot is then given by

$$I = -e \sum_{N_{\text{TOT}}} P_{N_{\text{TOT}}} (\langle \Gamma^1_{N_{\text{TOT}}N_{\text{TOT}}+1} \rangle - \langle \Gamma^1_{N_{\text{TOT}}N_{\text{TOT}}-1} \rangle), \quad (4)$$

where the angular brackets in the rates denote

$$\langle \Gamma^{1(2)}_{N_{\text{TOT}}N_{\text{TOT}}+1} \rangle \equiv \sum_{ij} g_{\text{eq}N_{\text{TOT}}i} \Gamma^{1(2)}_{N_{\text{TOT}}iN_{\text{TOT}}+1j}, \qquad (5)$$

and

$$\langle \Gamma^{1(2)}_{N_{\text{TOT}}+1N_{\text{TOT}}} \rangle \equiv \sum_{ij} g_{\text{eq}N_{\text{TOT}}+1i} \Gamma^{1(2)}_{N_{\text{TOT}}+1iN_{\text{TOT}}j}. \qquad (6)$$

In the Eqs. (5) and (6) $\Gamma^{1(2)}_{N_{\text{TOT}}+1iN_{\text{TOT}}j}$ and $\Gamma^{1(2)}_{N_{\text{TOT}}iN_{\text{TOT}}+1j}$ are the tunneling rates of a quasiparticle in the ith excited state

from the $N_{\text{TOT}}+1$-excess-electron double dot through the first or second junction, leaving the double dot with N_{TOT} excess electrons in one of its jth excited states, and similarly for the reverse process. These rates are calculated using the Fermi golden rule:

$$\Gamma^{1(2)}_{N_{\text{TOT}}iN_{\text{TOT}}+1j} = \frac{2\pi}{\hbar} \sum_\alpha |\langle N_{\text{TOT}}+1j|t^{1(2)}{}_\alpha c^\dagger{}_{1(2)\alpha}|N_{\text{TOT}}i\rangle|^2$$
$$\times \rho^{1(2)}(F^0_{N_{\text{TOT}}+1j} - F^0_{N_{\text{TOT}}i} - eV_{1(2)})$$
$$\times f(F^0_{N_{\text{TOT}}+1j} - F^0_{N_{\text{TOT}}i} - eV_{1(2)}), \qquad (7)$$

$$\Gamma^{1(2)}_{N_{\text{TOT}}iN_{\text{TOT}}-1j} = \frac{2\pi}{\hbar} \sum_\alpha |\langle N_{\text{TOT}}i|t^{1(2)}{}_\alpha c^\dagger{}_{1(2)\alpha}|N_{\text{TOT}}-1j\rangle|^2$$
$$\times \rho^{1(2)}(F^0_{N_{\text{TOT}}i} - F^0_{N_{\text{TOT}}-1j} - eV_{1(2)})(1$$
$$-f(F^0_{N_{\text{TOT}}i} - F^0_{N_{\text{TOT}}-1j} - eV_{1(2)}). \qquad (8)$$

In Eqs. (7) and (8) $\rho^{1,2}$ is the density of states in the leads, which we take to be energy independent. The Fermi-Dirac distribution function $f(\Delta)$ gives the probability to find a quasiparticle in the lead at the energy $\Delta = F^0_{N_{\text{TOT}}i} - F^0_{N_{\text{TOT}}-1j} - eV_{1(2)}$. The equilibrium probability $g_{\text{eq}N_{\text{TOT}}i}$ to find a N_{TOT} excess electron double dot in one of its ith excited states is given in the canonical ensemble by

$$g_{\text{eq}N_{\text{TOT}}i} = \frac{\exp{-\beta F^0_{N_{\text{TOT}}i}}}{\sum_i \exp{-\beta F^0_{N_{\text{TOT}}i}}}, \qquad (9)$$

where $F^0_{N_{\text{TOT}}i}$ is the ith excited state energy of the operator $\hat{F}^0$ in Eq. (2) evaluated in the Hilbert space of N_{TOT}.

Using Eqs. (1)–(9) we calculate the nonlinear current through the double dot. In particular, the Coulomb gap ΔV_{gap} and the normalized peak splitting[1] f defined as the ratio of the additional energy needed to increase the number of quasiparticles by one to its maximum (saturation) value are, respectively, given by (with the total number of particles being 1 or 2)

$$\Delta V_{\text{gap}} = 4\left[\frac{(2-b_2)(u_{11}+\varepsilon_1) - \sqrt{b_1^2(u_{11}+\varepsilon_1)^2 + [(2-b_2)^2 - b_1^2]t^2}}{[(2-b_2)^2 - b_1^2]}\right], \qquad (10)$$

$$f = [u_{11} + u_{12}/2 + 2t - \sqrt{(u_{11}-u_{12}/2)^2 + 2t^2}]/(U/2), \qquad (11)$$

where u and t are those appearing in the Mott-Hubbard model defined through Eqs. (1)–(3), U is the intradot interaction energy of the isolated dot, $b_1 = x_{b1} - x_{b2}$ and $b_2 = x_{b1} + x_{b2}$. Thus a knowledge of the Mott-Hubbard parameters u_{11}, u_{12}, t, etc. allows us to obtain the complete current-voltage characteristics of the double-dot system within our simple molecular-orbital-type phenomenological model.

III. A MICROSCOPIC MODEL FOR ESTIMATION OF HUBBARD PARAMETERS

We construct a simple microscopic quantum-mechanical model to phenomenologically describe the double-dot system depicted in the left inset of Fig. 1 at $V=0$, $V_g=0$. [Within our model the finite bias and gate voltages are accounted for in the Hamiltonian in Eq. (2).] Our microscopic confinement model is shown as the right inset of Fig. 1. The model uses two identical one dimensional infinite hard wall potential wells to describe the single-particle states ψ_α in the

two isolated dots. Each dot is represented by a two-step well (as shown in Fig. 1) with the lower step well of width a (a region where ψ_α are quasilocalized) representing the intradot interaction energy of the individual dot, and the rectangular barrier of potential height V_b and width d representing the (variable) tunnel barrier separating the two dots. When the barrier V_b is large (e.g., $V_b \to \infty$) the tunnel conductance is vanishingly small and the two dot system is in the uncoupled "atomic" limit whereas for small V_b (e.g., $V_b \to 0$) the dimensionless "tunnel" conductance approaches unity and the system is in the composite "molecular" limit. When the barrier becomes "transparent" and no single-particle state α satisfying $\varepsilon_\alpha < V_b$ exists, the model breaks down. Within our one-dimensional confinement model the barrier of height V_b and width d approximates the intradot constriction. Such simple one dimensional potential confinement models have earlier been used[11] to study quantum tunneling characteristics in three-dimensional systems. We emphasize that our microscopic one dimensional quantum confinement model should be taken as a simple phenomenological (rather than a realistic) description of the experimental double-dot system.

We evaluate the Mott-Hubbard interaction parameters u_{11} and u_{12} by taking the expectation values of the screened Coulomb interaction using the potential confinement model for the lowest single-particle states in each dot. We take the Thomas-Fermi form of the screened Coulomb potential V_c with the screening length as 220 Å. The short-ranged part of the Coulomb interaction is assumed unscreened and is approximated by a δ function potential. The form of the screened Coulomb potential in the experimental system containing many electrodes is *a priori* unknown. We, therefore, treat the form of the screened Coulomb potential as an adjustable fitting parameter for phenomenological convenience. Within our simplistic confinement model such a phenomenological approach is reasonable. Then the intradot (interdot) u_{11} (u_{12}) energy is given by the overlap integral of the Coulomb potential evaluated between states of the same (different) dots:

$$u_{11} = \frac{1}{2} \int \int dy \, dx \, \psi_1^2(x) V_c(|x-y|) \psi_1^2(y), \quad (12)$$

$$u_{12} = \frac{1}{2} \int \int dy \, dx \, \psi_1^2(x) V_c(|x-y|) \psi_2^2(y). \quad (13)$$

The hopping parameter t can be defined in several alternative ways within our microscopic model. We evaluate t as $t = \Delta_{\text{sas}}/2$, where Δ_{sas} is the so-called symmetric-antisymmetric energy gap between the two lowest single-particle energy levels in our model double-well potential. Conduction in the coupled dot system occurs through a single spin-degenerate quasiparticle state $\psi_{1\text{dot}}$ at the ground-state energy ε_1 of the potential well. Finally, we need to evaluate the interdot conductance g within our microscopic model in order to make direct contact between the experimental[1-3] (and earlier theoretical[4,5]) results and our model calculations. The interdot conductance g can of course be exactly evaluated for our simple one-dimensional rectangular barrier model of the point contact separating the two dots. Because of our hard-wall potential confinement model, however, the exactly calculated ("hard") conductance for a

tunnel barrier of height V_b and width d is a rather poor approximation (even on a qualitative level) for the experimental interdot point contact conductance. We have, therefore, employed a "soft" conductance approximation using a WKB expression, $g \approx \exp\{-2[(2md^2/\hbar^2)(V_b - \varepsilon_1)]^{1/2}\}$, which we believe better represents (on a qualitative level) the adiabatic confinement potential expected in the experimental double-dot system. We find much better qualitative agreement between our theory and experiment using the "soft" conductance model, which is what we will mostly present in this paper.

Within our highly simplified microscopic model for the double-dot system, the gate-voltage-induced lowering of the interdot barrier V_b causes the crossover from two isolated dots (for large V_b) of size a each separated by a distance d to a single composite coherent double dot (for small V_b) of size $2a + d$. Thus a single tunable parameter V_b controls the "transparency" of the system and causes the transition. Instead of using V_b as the control parameter, however, we follow the experimental procedure of using the interdot tunnel conductance g (determined completely by V_b in the "soft" and "hard" approximations as described above) as the control parameter in depicting our results. As V_b is tuned all the parameters of our model (e.g., $t, \varepsilon_1, u_{11}, u_{12}, g$) vary as known functions of V_b. We fix the individual dot size a (≈ 350 nm) using the experimental[1] value of the intradot interaction energy $u_{11} \approx 230$ μeV for the isolated dot. To compare our model to experiments we take the width of the barrier d to be 10 times smaller than a. There is no particular significance to this choice of $a = 10d$ except that we expect the individual dot size to be substantially larger than the barrier region.

Our calculated Hubbard model parameters (e.g., $\varepsilon_1, t, u_{11}, u_{12}$) are shown as functions of the corresponding interdot soft conductance g in Fig. 1. Although u_{11} and u_{12} approach each other as g increases, the simplicity of our microscopic model does not produce $u_{11} = u_{12}$ for $g = 1$. This is mainly due to the various approximations used in calculating the overlap integrals for the Coulomb energy. This discrepancy is the most severe quantitative limitation of our model.

We formulated our model in terms of interactions u_{11} and u_{12}, which together define the value of the total capacitance $C_\Sigma = C_0 + C_g + C + C_{\text{int}}$ of each dot and the value of the interdot capacitance C_{int}. This leaves the ratio C_g / C_0 undetermined. We assume it to remain fixed during the merging transition, and set it to its experimental value $C_g / C_0 \approx 0.1$ when the two-dot system is in the "atomic limit."

IV. LINEAR CONDUCTANCE

A. Double-dot peak splitting and Coulomb gap

In Fig. 2 we show our calculated Coulomb blockade oscillations for the double-dot system (in the linear regime) for four values of the soft interdot conductance $g = 0.16$, 0.52, 0.8, and 0.99 at $T = 87$ mK ($k_b T \ll u_{11}$). Note that for the sequential tunneling situation considered here, the width of the Coulomb blockade peaks arises entirely from thermal broadening. Our calculated evolution of the Coulomb blockade oscillations from the degenerate single-dot oscillations
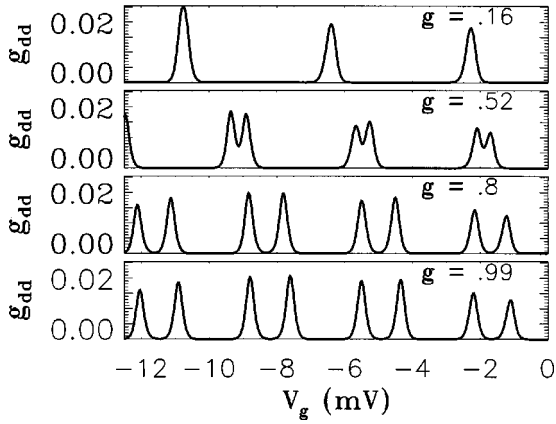
FIG. 2. The conductance g_{dd} in units of e^2/h through the double-quantum-dot system versus the gate voltage V_g for four values of the soft interdot conductance $g = 0.16$, 0.52, 0.8, and 0.99 at $T = 87$ mK in the linear regime ($V_{sd} = 10 \mu$eV). We use $\varepsilon_2/\varepsilon_1 = 2$, $t_2/t_1 = 1.2$, and $t_2^{1,2}/t_1^{1,2} = 1.2$ for the single-particle spin degenerate levels.

(at low g) through peak splitting (intermediate g) to the eventual period doubling (at large g) of the Coulomb blockade oscillations is qualitatively similar to experimental observations (cf. Fig. 5 of Ref. 1). To further quantify our results we show in Fig. 3 our calculated normalized peak splitting f [Eq. (10)] and the Coulomb gap ΔV_{gap} [Eq. (11)] as functions of the interdot tunnel conductance g, both for soft and hard conductance models. The corresponding experimental data[1] for f show considerable scatter and our results (for the soft model) agree with experiment. The hard model, however, disagrees with the experimental results for reasons discussed above. We point out that the main quantitative limitation of our model seems to be a weaker (stronger) dependence of both f and ΔV_{gap} on the tunnel conduc-
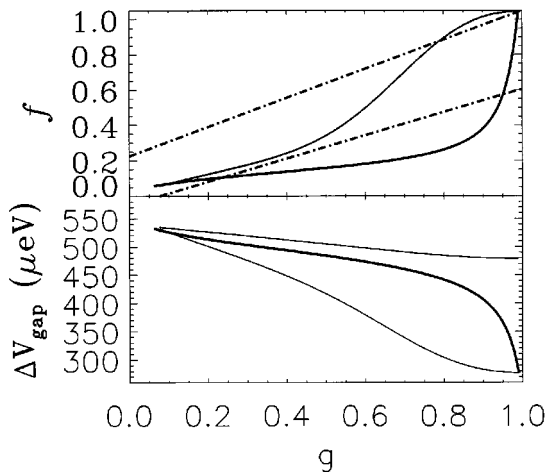
FIG. 3. Calculated normalized peak splitting f [Eq. (11)] and the Coulomb gap ΔV_{gap} [Eq. (10)] as functions of the interdot tunnel conductance g (top and bottom panels) for soft and hard (thick lines) conductance models. The dashed lines show the boundaries for the scatter of the experimental data (taken from Fig. 5 of the second paper in Ref. 1). The top thin line in the bottom panel shows the Coulomb gap for *fixed* values of ΔV_{gap} with $u_{11} = 227 \mu$eV and $u_{12} = 0.11 \mu$eV.

tance g for small (large) values of g than seen in experiments. We want to emphasize here that due to the various (somewhat arbitrary) approximations that we use to calculate *a priori* unknown phenomenological parameters in our microscopic model, we do not expect to get quantitative agreement with the experimental results that the perturbative theories obtain[4,5] [for g, $(1-g) \ll 1$]. The experiments were apparently carried out in the regime of more than one single-particle state per interdot conducting channel, making the continuum description of Refs. 4 and 5 appropriate for the calculation of f. However, our model suggests a mechanism for the merging of two dots into one composite dot in the limit of one single-particle state per conducting channel—a situation that cannot be covered by the perturbative theories. In principle, experiments can be performed in the regime we study, namely, when there is only one single-particle state per conducting channel. Our calculated normalized splitting f in Fig. 3 shows a qualitative agreement with the experimental data, suggesting that even the extreme limit studied by us may be germane to real systems.

We should also note that the assumption that intradot and interdot interaction energies are fixed at values of isolated dots is inadequate within our model, as we find a small variation of the Coulomb gap calculated for this situation (see the bottom panel of Fig. 3).

B. Temperature dependence of linear conductance

In the linear bias voltage regime at charge degeneracy points $[F_0^0(N_{\text{TOT}}) = F_0^0(N_{\text{TOT}}+1)]$, the two states with N_{TOT} and $N_{\text{TOT}}+1$ give the dominant contribution to conductance, and the expression for current reduces to

$$I = -e \sum_{N_{\text{TOT}}} \frac{\langle \Gamma^1_{N_{\text{TOT}}N_{\text{TOT}}+1} \rangle \langle \Gamma^2_{N_{\text{TOT}}+1N_{\text{TOT}}} \rangle}{\langle \Gamma^1_{N_{\text{TOT}}N_{\text{TOT}}+1} \rangle + \langle \Gamma^2_{N_{\text{TOT}}+1N_{\text{TOT}}} \rangle}. \quad (14)$$

For thermal energy smaller (larger) than the level separation (the width of transmission resonance) in a double-dot the conductance formula reduces to a single-dot result:[10]

$$g_{dd} = -e^2 \sum_{N_{\text{TOT}}} \frac{\Gamma^1_{N_{\text{TOT}}N_{\text{TOT}}+1} \Gamma^2_{N_{\text{TOT}}+1N_{\text{TOT}}}}{\Gamma^1_{N_{\text{TOT}}N_{\text{TOT}}+1} + \Gamma^2_{N_{\text{TOT}}+1N_{\text{TOT}}}} f'[F_0^0(N_{\text{TOT}}+1)$$
$$- F_0^0(N_{\text{TOT}})]. \quad (15)$$

Thus the height of a conductance peak is inversely proportional to temperature, the width is linear in temperature, and the line shape is given by the inverse hyperbolic cosine squared, i.e.,

$$g_{dd} \sim \frac{1}{kT} \cosh^{-2}\left(\frac{F_0^0(N_{\text{TOT}}+1) - F_0^0(N_{\text{TOT}})}{2kT} \right).$$

This fairly strong temperature dependence of the linear conductance is a direct result of our assumption of one single-particle state per conducting channel in our Mott-Hubbard molecular orbital model—by contrast, the perturbative theories[4,5] with a continuum of states predict extremely weak temperature dependence.

We show in Fig. 4 the directly numerically calculated Coulomb blockade oscillations for $g = 0.16$ and $g = 0.8$ for several temperatures in our theory. Note that the double-peak
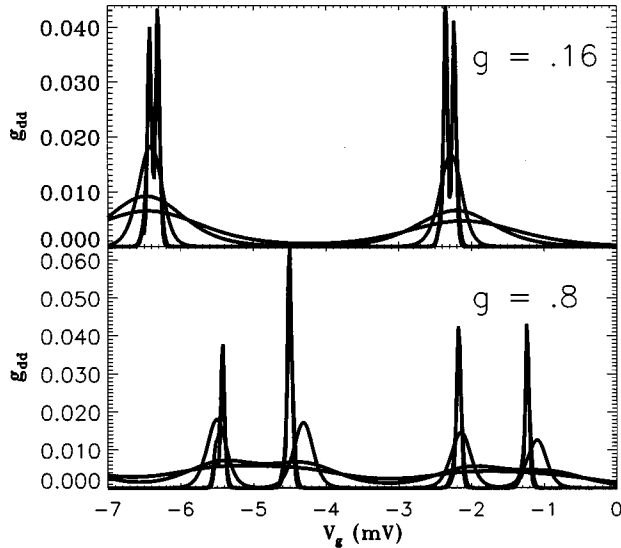
FIG. 4. The conductance g_{dd} versus the gate voltage V_g for two values of the soft interdot conductance $g = 0.16$ (upper panel) and $g = 0.8$ (lower panel) is shown for $T = 20, 30, 100, 400$, and 600 (mK) temperatures from top to bottom in each panel.

splitting is not resolved in Fig. 4 when $2kT \approx F_0^0(N_{TOT} + 1) - F_0^0(N_{TOT}) \sim u_{12} + 2t$. The temperature dependence of peak widths in Fig. 5(a) is described rather
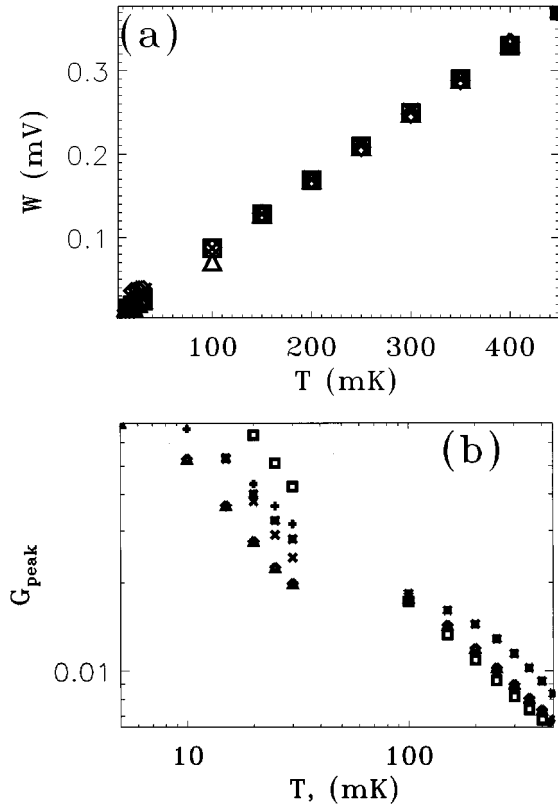
FIG. 5. The widths W (a) and the heights G_{peak} (b) of the conductance peaks at charge degeneracy points $F_0^0(N_{TOT} = 2) = F_0^0(N_{TOT} = 3)$ for soft $g = 0.16$ (pluses), $g = 0.8$ (squares), and $g = 0.92$ (triangles); and at $F_0^0(N_{TOT} = 3) = F_0^0(N_{TOT} = 4)$ for $g = 0.16$ (asterisks), $g = 0.8$ (X), and $g = 0.92$ (diamonds) as a function of temperature.
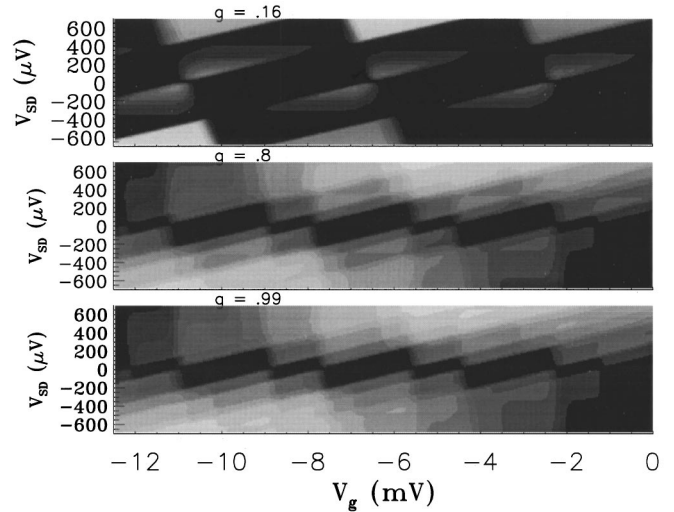
FIG. 6. The nonlinear current I through the double-dot system (at $T = 87$ mK) is plotted versus the values of the gate voltage V_g and the bias voltage V_{SD} for three values of the interdot soft conductance $g = 0.16, 0.8, 0.99$. The brightest shades in the plots correspond to $I = 59, 76$, and 78 pA for the graphs from top to bottom. The states with $N = 0$ to $N = 8$ electrons in the double-dot system contribute to I in the shown parameter space.

well by Eq. (15), i.e., $W = 2kT/x_g$. The slope of the temperature dependence of W in Fig. 5(a) is given by x_g (and therefore by the ratio C_g/C_0) which remains approximately unchanged during the transition to the composite system. In agreement with our theoretical results as shown in Fig. 5(a) the experimentally observed[1] temperature dependence of the peak widths is also linear in temperature.

As expected for a finite number of single-particle states participating in the conduction through the double-dot, the conductance peak heights are suppressed in Fig. 5(b). Experimentally the peak suppression is seen, but is not as strong as that predicted by Eq. (15). The experimentally observed peak height suppression indicates that for a range of temperatures the experiments[1,2] might have been performed in the regime where a finite number of states per conducting channel participate in tunneling. The continuum description[4,5] predicts no suppression of the conductance peak height, in contrast to the experimental observation.

V. NONLINEAR SEQUENTIAL TUNNELING CURRENT

Finally, in Fig. 6 we show for $g = 0.16, 0.8$, and 0.99 our calculated nonlinear Coulomb blockade transport characteristics for the double-dot system by plotting the calculated current (in gray scales) as a function of both the source-drain voltage and the gate voltage. Again, our results are in good qualitative agreement with the experimental data[2] with the main quantitative discrepancy arising from the inadequacy in our tunnel conductance value g, which is relatively higher than the corresponding experimental result.

In Fig. 7 we show a familiar Coulomb blockade staircase structure at fixed values of gate voltage V_g in Fig. 6. Each new ground state of a double-dot with increased total number of excess charges by one adds a step in the current seen in this plot. The level separation between the excited states is comparable to thermal energy and is not resolved in Fig. 7.
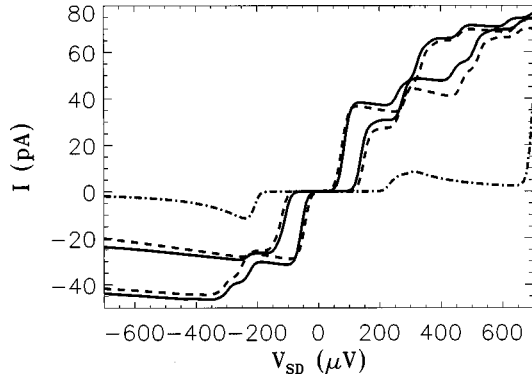
FIG. 7. Coulomb blockade staircase structure in I through the double-dot system (at $T = 87$ mK) is shown for fixed values of V_g at the centers of the linear bias regime stability regions in Fig. 6 of a double dot with $N_{TOT} = 2$ and $N_{TOT} = 3$ excess charges for three values of the interdot soft conductance $g = 0.16$ (dash dotted line), $g = 0.8$ (dashed line), and $g = 0.99$ (solid line).

Overall our calculated nonlinear transport characteristics are in reasonably good qualitative agreement with the experimental observations.

VI. SUMMARY

In conclusion, using a simple single-parameter (V_b) one-dimensional microscopic confinement model we calculate *nonperturbatively* the linear and nonlinear Coulomb blockade characteristics of a double dot system as a function of the interdot tunnel conductance. Our results are in reasonable qualitative agreement with the experimental results. We can obtain better quantitative agreement with experiment by using additional (e.g., d and a) adjustable parameters in a two-dimensional depiction of a double dot, or by including the dependence of all the Mott-Hubbard parameters on the excited single-particle states in each dot, as well as by using more refined definitions of the form of the screened Coulomb potential, but we feel that such ''improvements'' are not particularly meaningful within our simple model. Our approach to nonlinear transport in the double-dot system for arbitrary interdot coupling strengths gives a physical justification to the variation of all the model parameters with the strength of the interdot coupling alluded to in the classical charging models,[1] without sacrificing the important charge fluctuation effects that are the main feature of the existing weak and strong coupling perturbative quantum theories.[4,5]

We have emphasized throughout that our Mott-Hubbard Hamiltonian-based molecular-orbital approach is *complementary* to the perturbative charge fluctuation theory developed earlier in Refs. 4 and 5. The perturbative calculations incorporate a continuum of states whereas we have a finite number (actually, one) of states per conducting channel. The perturbative theory is exact for small g (or $1 - g$) whereas the various uncontrolled approximations we use in calculating our Mott-Hubbard parameters render our theory quantitatively not particularly reliable in any limits. On the other hand, our calculation is nonperturbative and can be used to calculate nonlinear transport characteristics through the double-dot system. The fact that our calculated temperature dependence of linear conductance is in reasonable agreement with experimental observations (the continuum perturbative theories predict negligible temperature dependence) suggests that, at least in some temperature regime, the experimental double dot system most likely is in an intermediate region in between the two theoretical limits of many states per conducting channel[4,5] and just one state per channel as we use in our Mott-Hubbard description. We note that it is, in principle, possible[6] for us to include more than one state per channel in our numerical calculations, but for reasons already discussed it is unclear that such a calculation is a meaningful improvement within our simple model. We believe that the most significant feature of our theory is the explicit demonstration that a simple molecular-orbital-type model is capable of providing a good qualitative description for the linear and nonlinear transport properties of a double-quantum-dot system over a wide range of bias voltage and temperature.

[1] F. R. Waugh *et al.*, Phys. Rev. Lett. **75**, 705 (1995); F. R. Waugh *et al.*, Phys. Rev. B **53**, 1413 (1996).

[2] C. H. Crouch *et al.*, Surf. Sci. **361/362**, 631 (1996); C. H. Crouch, Ph.D. thesis, Harvard University, 1996.

[3] C. Livermore *et al.*, Superlattices Microstruct. **20**, 633 (1996).

[4] K. A. Matveev, L. I. Glazman, and H. U. Baranger, Phys. Rev. B **53**, 1034 (1996); **54**, 5637 (1996).

[5] J. M. Golden and B. I. Halperin, Phys. Rev. B **53**, 3893 (1996); **54**, 16 757 (1996).

[6] C. A. Stafford and S. Das Sarma, Phys. Rev. Lett. **72**, 3590 (1994); Phys. Lett. A **230**, 73 (1997).

[7] G.-L. Chen, G. Klimeck, S. Datta, G.-U. Chen, and W. A. Goddard III, Phys. Rev. B **50**, 2316 (1994); **50**, 8035 (1994).

[8] R. Kotlyar and S. Das Sarma, Superlattices Microstruct. **20**, 641 (1996).

[9] P. Delsing, J. E. Mooij, and G. Schön, in *Single Charge Tunneling*, edited by H. Grabert and M. Devoret (Plenum, New York, 1992).

[10] C. W. J. Beenakker, Phys. Rev. B **44**, 1646 (1991).

[11] R. E. Prange, Phys. Rev. **131**, 1083 (1963).